RESEARCH ARTICLE

Proteome analysis and characterization of phenotypes of lesion mimic mutant *spotted leaf 6* in rice

Sang Gu Kang[1], Mohammad Nurul Matin[1], Hanhong Bae[2] and Savithiry Natarajan[3]

[1] Molecular Genetics Laboratory, School of Biotechnology, Institute of Biotechnology, Yeungnam University, Gyeongsan, Korea
[2] US Department of Agriculture, Agricultural Research Service, Sustainable Perennial Crops Laboratory, PSI, Beltsville, MD, USA
[3] US Department of Agriculture, Agricultural Research Service, Soybean Genomics and Improvement Laboratory, PSI, Beltsville, MD, USA

Rice *spotted leaf 6* (*spl6*) mutant produces lesions caused by spontaneous cell death in the absence of pathogenic infection. Expression of this genetic trait was developmentally programmed. After the tillering stage, small red and brown lesions were initiated in groups on the leaf blade. Eventually, the lesions formed parallel lines along the midrib of the leaf. Under light and transmission electron microscopy, we observed that thylakoid membranes of mesophyll chloroplasts were progressively damaged in the nonspotted section of the mutant leaf. However, chloroplasts were absent in the mesophyll cells of the spotted area of the *spl6* mutant. These results indicated that lesion formation of the *spl6* mutant might be caused by oxidative burst. Proteome analysis revealed that 159 protein spots were up or downregulated in comparison between spotted leaves of the *spl6* mutant plants and normal leaves of the wild type. Among them, protein disulfide isomerase (PDI), transketolase, thioredoxin peroxidase (TPX), ATP synthase, RuBisCO large subunit, and RuBisCO activase small subunit were not identified in the *spl6* mutant but were abundant in the wild type. Especially, the absence of TPX and PDI might be the cause of the failure to protect cells against oxidative burst resulting in degradation of the thylakoid membranes and leading to programmed cell death and lesion development.

Received: December 2, 2006
Revised: March 30, 2007
Accepted: April 8, 2007

Keywords:
Lesion mimic mutant / Lesion resembling disease (*lrd*) / *Oryza sativa* / Programmed cell death

Correspondence: Dr. Sang Gu Kang, Molecular Genetics Laboratory, School of Biotechnology, Institute of Biotechnology, Yeungnam University, Gyeongsan 712-749, Korea
E-mail: kangsg@ynu.ac.kr
Fax: +82-53-816-8498

Abbreviations: *lrd,* lesion resembling disease; **PCD,** programmed cell death; **PDI,** protein disulfide isomerase; **PGK,** phosphoglycerate kinase; **RuBisCO-ACS,** ribulose-1,5-bisphosphate carboxylase/oxygenase activase small isoform; **RuBisCO-L,** RuBisCO large chain; ***spl6,*** spotted leaf 6; **TEM,** transmission electron microscopy; **TK,** transketolose; **TPX,** thioredoxin peroxidase

1 Introduction

Plants are exposed to various kinds of abiotic and biotic stresses, as well as mechanical damage throughout their life cycle. In plants, ROS such as superoxide (O_2^-), hydrogen peroxide (H_2O_2), and hydroxyl radical ($^{\bullet}OH$) are produced by environmental stresses and as by-products of normal biochemical processes [1]. These ROS cause malfunctions in cellular metabolism and membrane structure [2]. Plants induce several physiological and structural adjustments to detoxify the ROS and to protect themselves from stresses

including pathogen attack. Plants also can activate genetic resistances to protect themselves from stresses induced by pathogenic elicitors [3]. To activate resistance against a specific pathogen, the presence of a specific allele of the resistant gene is required. In some cases, plants protect themselves from stresses by creating a response against the stress elicitors through programmed cell death (PCD) which is spontaneous death of localized cells [4, 5]. This PCD is a physiological result of a plant hypersensitive response (HR) to pathogenic infection [6, 7].

In nature, some mutant plants show genetically autonomous cell death without pathogenic attack and create various kinds of spots on the leaves. These are called lesion mimic mutants or lesion resembling disease (*lrd*) mutants [3, 8, 9]. Such mutants have been identified in rice (*Oryza sativa*) [10], maize (*Zea mays*) [11], barley (*Hordeum vulgare*) [12], and *Arabidopsis* [7, 13]. These lesion mimic mutants share a unique lesion phenotype with callose deposition, inducible expression of defense-related genes, and increasing ROS substances in cells [14]. Several genes controlling lesion mimic phenotypes have been identified and characterized. In *Arabidopsis*, the *LSD1* gene encodes a novel protein containing three zinc finger domains and negatively regulates cell death by inhibiting signals from superoxide production [15]. In barley, the *Mlo* gene encodes plant-specific proteins containing a transmembrane-spanning helices domain which negatively regulates the cell death [16]. In maize, *Les22* encodes uroporphyrinogen decarboxylase which is necessary for chlorophyll biosynthesis and induces lesion resembling symptoms [17]. These identified genes of lesion mimic mutants have different functions but show similar lesion mimic phenotypes with *spotted leaf 6* (*spl6*) mutant and facilitate the plants to increase their resistance against stresses, as well as pathogens, through either accumulation of ROS or expression of defense related genes [12, 14, 15].

Currently, 25 lesion mimic mutants have been identified [10]. The rice *lrd* mutants have been grouped into the *spl* family, the *b*rown *l*eaf spot (*bl*) family, and the *z*ebra *n*ecrosis (*zn*) family [18, 19]. Among them, *spl11* [3], *spl1* [9], lesion mimic *cell death and resistance* (*cdr*) [20], and *blast lesion mimic mutants* (*blm*) [21] showed broad-spectrum resistance to rice blast fungus and bacterial blight. Because lesion-mimic genes are related to control of cell death in the pathogen-defense response, some genes causing the rice *lrd* mutants have been identified. For example, the *spl11* gene encodes a U-box/ARM protein and confers nonrace specific resistant to rice blast and bacterial blight [22]. The *spl7* gene encodes a heat stress transcription factor [5]. Although, a large family of *spl* alleles has been identified in rice, little work has been done to characterize the genetic functions of the *spl* genes.

The *spl6* gene causes early lesions at the tillering stage of rice. Tiny specks gradually increase into large lesions through continuous formation of new lesions and join together to form longitudinal lines of lesions through the leaf blade [19]. This pattern of lesion formation is different from that of other lesion mimic mutants. Although the *spl6* mutant shows a unique lesion mimic mutant phenotype, no molecular and cellular characterization of the *spl6* mutant has been done to date.

Proteome analysis is one of the direct approaches for finding functional proteins in quantitative and qualitative measurements. It provides a detailed assessment of physiological processes in the subjected cells or organs. Here, we characterized the phenotypes of the rice *spl6* mutant with proteome analysis to investigate the molecular mechanisms of lesion formation.

2 Materials and methods

2.1 Plant materials and phenotype analysis

A *spl6* mutant and wild-type rice (*O. sativa* L. Japonica cv. Ilpoom-byeo) were grown under natural field conditions between 30 and 35°C in 2006 in a paddy field of Yeungnam University, Gyeongsan, Korea. The data on spot formation time, color, shape, size, and arrangement, as well as severity of spot formation, were documented at different developmental stages. Fully developed and matured whole leaf blades from each plant were collected. The average length and width of the leaf blade samples were 50 and 1.3 cm, respectively. The leaf blade samples were immediately frozen in liquid nitrogen and stored at −80°C until sample preparation for proteomic and Northern blot analysis.

2.2 Microscopy

For the light microscopic study, thin sections (1.0 cm^2) of wild type, nonspotted and spl of the *spl6* mutant were cut using a sharp blade and were observed using an Olympus BX51 dissecting microscope (Olympus, Tokyo, Japan) under white light and UV light with a 488 nm emission filter. Photographs were taken using an Olympus C-7070 digital camera (Olympus).

For transmission electron microscopy (TEM) analysis, leaf segments (1 mm × 5 mm) were cut from the 90 days old developing and matured flag leaves of wild type, nonspotted and spotted part of *spl6* mutant. The samples were fixed with 2.5% v/v glutaraldehyde in a 0.1 M sodium phosphate buffer (pH 7.0) and incubated at 4°C with five buffer changes for 30 min intervals. The samples were then transferred to 4°C for 12 h. Following fixation, the samples were washed with 0.1 M sodium phosphate buffer, pH 7.0, for three 20 min incubations at 4°C. After washing, samples were postfixed for 6 h in 1% v/v osmium tetroxide in a sodium phosphate buffer (pH 7.0). After three buffer washes, the samples were dehydrated through a graded series of ethanol. After 15 min incubation in propylene oxide, the samples were further incubated in epoxy resin solution (0.46 M EMBED-818, 0.28 M nadic methyl anhydride, 0.25 M dodecenyl succinic anhydride, 17.2 mM 2,4,6-Tri(dimethylaminoethyl) phenol

in propylene oxide at 1:1 v/v volume) for 4 h at room temperature. The samples were then incubated in a 2:1 v/v epoxy resin solution for 12 h at room temperature. Samples were then embedded in fresh epoxy resin solution and polymerized overnight at 70°C. Ultrathin sections were prepared using an MT-X ultramicrotome (RMC, AZ, USA). Sections were viewed in an H-7600 transmission electron microscope (Hitachi, Japan) operated at 80.0 kV in the microscopic analysis center at the Center for Facility at Yeungnam University, Korea. Three biological replicates using leaf blades from each of the three different plants were used for all microscopic analyses.

2.3 Protein extraction

For protein extraction, fully developed and matured leaf blades of 90 days old plants of *spl6* mutant and wild-type plant (Ilpoom byeo) were used. Each of the proteins was extracted independently twice from the leaf blades of the each two different plants. Frozen leaf samples were ground to fine powder with liquid nitrogen and the tissue powder was homogenized directly by mortar-driven homogenizer (PowerGen125, Fisher Scientific, Springfield, NJ, USA) in an extraction buffer containing 7 M urea/2 M thiourea; 4% w/v 3-[(3-cholamidopropyl)dimethylammonio]-1-propane-sulfonate (CHAPS); 1% w/v DTT, and 2% v/v pharmalyte (pH 3.5–10.0, Amersham BioSciences, Piscataway, TX, USA) and 1 mM benzamidine. Proteins were extracted for 1 h at room temperature with vortexing. After centrifugation at $15\,000 \times g$ for 1 h at 15°C, insoluble material was discarded and soluble fraction was used for 2-DE. The concentration of protein was determined by the Bradford method [23] using a commercial dye reagent from BioRad Laboratories (Hercules, CA, USA).

2.4 2-DE and image analysis

Extracted proteins were analyzed by 2-DE and repeated twice independently using proteins from each of the two different samples. IPG dry strips (pH 4–10 NL and 24 cm in length, Genomine, Korea) were equilibrated for 12–16 h with 7 M urea, 2 M thiourea containing 2% w/v CHAPS, 1% v/v DTT, 1% v/v pharmalyte (pH 3.5–10.0, Amersham BioSciences), and respectively loaded with 200 μg of sample. IEF was performed at 20°C using a Multiphor II electrophoresis unit and EPS 3500 XL power supply (GE Healthcare, Piscataway, NJ) following the manufacturer's instructions. For IEF, the voltage was linearly increased from 150 to 3500 V during 3 h for sample entry followed by constant 3500 V, with focusing complete after 96 kV·h. Prior to the second dimension, strips were incubated for 10 min in equilibration buffer (50 mM Tris-Cl, pH 6.8, containing 6 M urea, 2% SDS, 1% DTT, and 30% glycerol). The strip was then transferred to an alkylation buffer (2.5% iodoacetamide, 6 M urea, 2% SDS, 30% glycerol, 50 mM Tris-HCl, pH 6.8). Equilibrated strips were inserted onto SDS-PAGE gels (20×24 cm, 10–16% gradient SDS gel). SDS-PAGE was performed using Hoefer DALT 2D system (GE Healthcare) following the manufacturer's instructions. The 2-D gels were run at 20°C for 1.7 kV·h and were then stained with silver nitrate (Sigma Chemical, St. Louis, MO) as described by Oakley *et al.* [24] but the fixing and sensitization step with glutaraldehyde were omitted. Stained gels were scanned using an ImageScanner II (Amersham BioSciences) in transmission mode. The p*I* and molecular mass (MM) of each spot were determined using 2-DE markers (GE Healthcare).

Quantitative analyses of digitized images were carried out using the PDQuest software (version 7.0, BioRad, Richmond, CA, USA) according to the protocols provided by the manufacturer and then manual editing was carried out. After spot detection, the quantity of each spot volume was normalized by total valid spot intensity. The spots displaying significant changes were considered to be differentially expressed proteins. Standard error was calculated from the spots of the gels from two independent experiments and used as error bars. Protein spots were selected based on the significant differences of spots quantities between the mutant and the wild type.

2.5 Enzymatic digestion of protein in-gel

Twenty-five protein spots, which displayed more than a two-fold variation of expression between wild type and mutant, were excised from the stained gels and digested according to Shevchenko *et al.* [25] using modified sequencing grade porcine trypsin (Promega, Medison, WI, USA). Gel pieces were washed with 50% ACN (Wako, Osaka, Japan) to remove SDS, salt, and stain and dried under vacuum to remove solvent and then rehydrated with trypsin (8–10 ng/μL, sequencing grade, Promega) solution by incubation for 8–10 h at 37°C. The proteolytic reaction was terminated by addition of 5 μL of 0.5% TFA. Tryptic peptides were recovered by combining the aqueous phase from several extractions of gel pieces with 50% aqueous ACN. After concentration, the peptide mixture was desalted using C_{18}ZipTips (Millipore Billerica, MA, USA), and peptides were eluted in 1–5 μL of ACN. An aliquot of this solution was mixed with an equal volume of a saturated solution of CHCA in 50% aqueous ACN and 1 μL of the mixture was spotted onto a target plate.

2.6 MALDI-TOF-MS analysis and database search

Protein analysis was performed using Ettan MALDI-TOF (GE Healthcare). Peptides were evaporated with a N_2 laser at 337 nm, and using a delayed extraction approach. They were accelerated with 20 kV injection pulse for TOF analysis. Each spectrum was the cumulative average of 300 laser shots. The Rockefeller University developed search program ProFound (http://129.85.19.192/profound_bin/ WebProFound.exe) was used for protein identification by PMF. Spectra were calibrated with trypsin autodigestion ion peak m/z (842.510, 2211.1046) as internal standards. Public databases including

ExPASy (http://www.expasy.org/), PROSITE (http://www.expasy.org/prosite/), BLAST (http://www.ncbi.nlm.nih.gov/BLAST/), BRENDA (http://www.brenda.uni-koeln.de/), and KEGG (http://www.genome.ad.jp/kegg/kegg2.html) were used for the database search.

2.7 Cloning cDNAs

Several cDNAs were cloned by the standard reverse transcription (RT)-PCR using a Universal Riboclone® cDNA Synthesis kit (Promega) according to the manufacturer's instructions. Primers were designed using the peptide sequence information obtained from the proteomic analysis and were used for RT-PCR (Table 1). Thermal cycling conditions using Taq DNA polymerase (Promega) were as follows: denaturing at 95°C for 2 min, followed by 29 cycles of denaturing at 95°C for 1 min, annealing at 55°C for 2 min and extension at 72°C for 2 min, and one cycle of extension at 72°C for 5 min. PCR products were cloned into pGEM-T Easy vector (Promega). Nucleotide sequencing was performed by the Bigdye 3.1 termination method using an ABI 3700 DNA analyzer (Applied Biosystem, Hitachi) at the Institute of Biotechnology, Yeungnam University.

2.8 Northern blot analysis

Northern blot analysis was performed according to Kang *et al*. [26]. Briefly, 20 μg of total RNA was electrophoretically separated on 1.4% denaturing agarose gel using 1× MOPS buffer and transferred to Nytran® nylon membranes (Schleicher & Schuell Bioscience, Keene, NH, USA) with 25 mM sodium phosphate buffer (pH 7.0) for 12 h. The membranes were exposed in UV at 1200 J. Radioactive labeled probes were generated from the PCR amplified ribulose-1,5-bisphosphate carboxylase/oxygenase large chain (RuBisCO-L), RuBisCO activase small isoform (RuBisCO-ACS), catalase (CAT), protein disulfide isomerase (PDI), and TPX genes by the random labeling system (Promega). Prehybridization was performed at 42°C for 3–4 h in 50% v/v formamide, 6× SSC (1× SSC is 0.15 M NaCl, 0.25 M NaH_2PO_4, and 25 mM Na_2EDTA), 5× Denhardt's solution (1% w/v Ficoll, 1% w/v PVP, 1% w/v BSA), 0.5% w/v SDS, and 0.1 mg/mL Herring sperm DNA. Hybridization was performed with α-[^{32}P] dCTP labeled probe at 42°C for 14 h. After hybridization, the membranes were washed twice in 2× SSC and 0.1% SDS solution at room temperature for 5 min, followed by washing in 1× SSC and 0.1% SDS solution at room temperature for 10 min, in 0.1× SSC and 0.1% SDS solution at room temperature for 20 min, and in 0.1× SSC and 0.1% SDS solution at 42°C for 5 min. Membranes were exposed for 24 h to X-ray film (Fuji photo film, Tokyo, Japan) for autoradiography. Northern blot analysis was carried out independently twice in this experiment.

3 Results

3.1 Phenotypes of *spl6* mutant

Four *spl6* mutant lines (YUM070, YUM110, YUM111, and YUM112) were found forming spontaneous lesions on the leaf blades from a previous study on lesion mimic *lrd* mutant alleles [19]. Among them, YUM111 was selected for further study. Figure 1 shows that in *spl6* mutant leaves, there were no visible spots on the leaves at the seedling stage (30 days), but spots appeared at the tillering stage (45 days) as very tiny specks and became clearly visible within 60 days under natural field conditions between 30 and 35°C. Interestingly, the flag leaf was severely covered by the spots resulting in earlier senescence than that of wild-type rice (Fig. 1A). The lesion formation in the *spl6* mutant was propagation type where lesions initiated sparsely at an early developmental stage but expanded rapidly to the entire leaf blade (Fig. 1B). As the formation progressed to a mature stage, a group of individual spots became attached together and eventually formed longitudinal lines through the minor leaf veins but rarely formed on major veins (Fig. 1B). Finally, the lesions occupied the whole leaf area resulting in early senescence.

Table 1. List of primers used in this study

Accession	Primers name	Sequences (5′-3′)
NM195989	OsRuBisCO-L, forward	723F, 5′-TGCGACTGCAGGTACATGCGA-3′
	OsRuBisCO-L, reverse	1410R, 5′-CTCGAACTCGAA TTTGATCGC-3′
AF052305	OsRuBisCO-ACS, forward	42F, 5′-CTCCGGCGTCCACTCCGACCA-3′
	OsRuBisCO-ACS, reverse	746R, 5′-GCGATGTCATCAGGGGCG-3′
DQ078758	OsCAT, forward	1F, 5′-ATGGATCCCTACAAGCACCGC-3′
	OsCAT, reverse	1478R, 5′-TTACATGCTCGGCTTCGCGCT-3′
AM039889	OsTPX, forward	1F, 5′-ATGGCCGCCTGCTGCTCCTCC-3′
	OsTPX, reverse	786R, 5′-TTAGATGGCCGCGAAGTACTC-3′
AY987391	OsPDI, forward	183F, 5′-CGTCGAGTTCTA CGCCCCGTG-3′
	OsPDI, reverse	987R, 5′-CAGCCCAAAGTACTGGAAGGC-3′

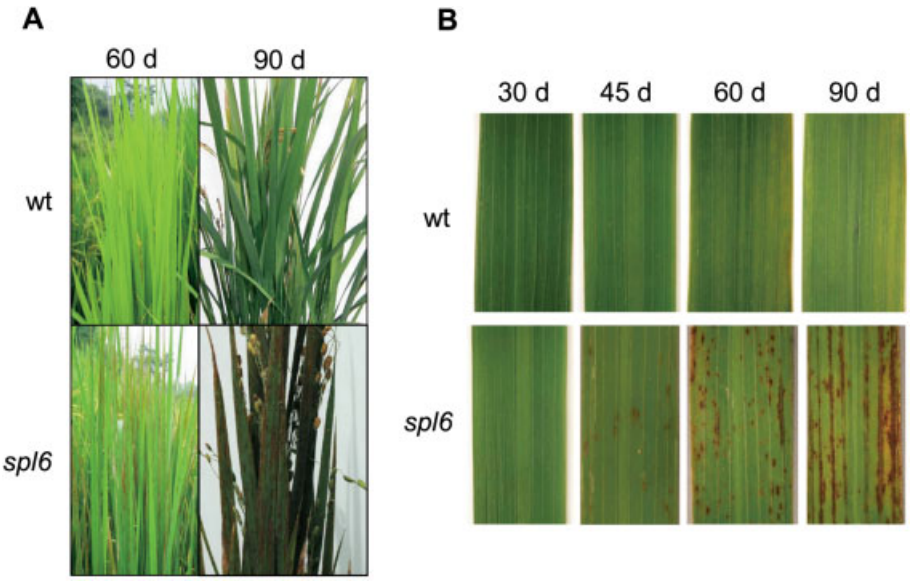

Figure 1. Phenotypes of wild type (wt) and *spl6* mutant. (A) 60 days (d) and 90 days old plant parts of wild type (wt) and *spl6*. (B) 30, 45, 60, and 90 days old leaves of wild type (upper panel) and *spl6* mutant (lower panel) with their phenotypes.

3.2 Leaf anatomical features of *spl6* mutant

Anatomical features of flag leaves of wild type and *spl6* mutant were observed under normal and fluorescent light using a light microscope (Fig. 2). Clear differences in the level of greenness of the mesophyll cells among wild type and mutant plants were found. In the sections of the wild-type leaf, as well as the nonspotted part of the mutant leaf, the mesophyll cells between the vascular bundles were green and filled with chloroplasts (Figs. 2A and B). In the spotted part of the *spl6* mutant leaf, however, the mesophyll cells were dark brown with very few greenish parts (Fig. 2C), indicating the death of the mesophyll cells. When we observed the cross-sections of leaves under the UV light at 488 nm, the color reflections of all three leaves showed clear differences (Fig. 2). The mesophyll cells of wild type and nonspotted part of mutant leaves were reddish, implying reflection of nonabsorbed light by the chloroplast, whereas mesophyll cells of spotted area of *spl6* mutant leaves did not turn red, indicating the degradation of the chloroplasts in the mesophyll cells (Figs. 2F and I).

To observe the presence or absence of chloroplasts and their ultra structure, we carried out TEM on the cross-sections of leaves of the wild type and the nonspotted and spotted areas of *spl6* mutant. We found clear differences in the structure of chloroplasts between leaves of wild type and *spl6* mutants. In wild-type leaves, well-developed mesophyll cells were found with fully developed chloroplasts (Figs. 3A, D, and G), whereas, in the section of nonspotted area of the mutant leaf, damaged chloroplasts with ruptured thylakoid membranes were found (Figs. 3B, E, and H). This indicates that those cells were beginning to die. Interestingly, the section from the spotted area of *spl6* mutant leaf showed that the chloroplasts in mesophyll cells were disappeared leaving a few ruptured thylakoid membranes in the cytoplasm (Figs. 3C, F, and I). In the magnified section of mutant leaves, some membrane-bound substances or plastoglobules were deposited in the cytoplasm which might be due to the accumulation of chemical substances or callose (Fig. 3F).

3.3 Proteome analysis between wild type and *spl6* mutant

Proteomic analysis was performed to test whether the proteins expression were different in wild type and *spl6* mutant leaves when lesions developed. Independently, two 2-D gels were carried out from the proteins of fully developed and matured leaf blades of wild type and mutant plants. Figure 4 shows representative images of 2-D gels. On the basis of these images, approximately 800 protein spots were reproducibly detected in gels with silver staining across the two biological replicates by manual editing after the automated detection and matching by PDQuest. However, 159 spots were expressed differentially between *spl6* mutant and wild-type leaf proteins. Among them, 114 protein spots were upregulated and 45 spots were downregulated between the *spl6* mutant and the wild-type leaf proteins, whereas 40 protein spots did not exist in the mutant leaf proteins compared with those of wild-type leaf proteins. Among the differentially expressed protein spots, 25 spots displayed more than a twofold variation as average intensities of the two replicates between the mutant and the wild type, which we selected for further MS analysis using an Ettan MALDI-TOF-MS (GE Healthcare) (Figs. 4A and B). A search program, ProFound, was used to compare the homology of the obtained proteins. Here, we discuss their functions and relation with *spl6* mutant. These identified protein spots represent ten different proteins with three unknown types and were categorized

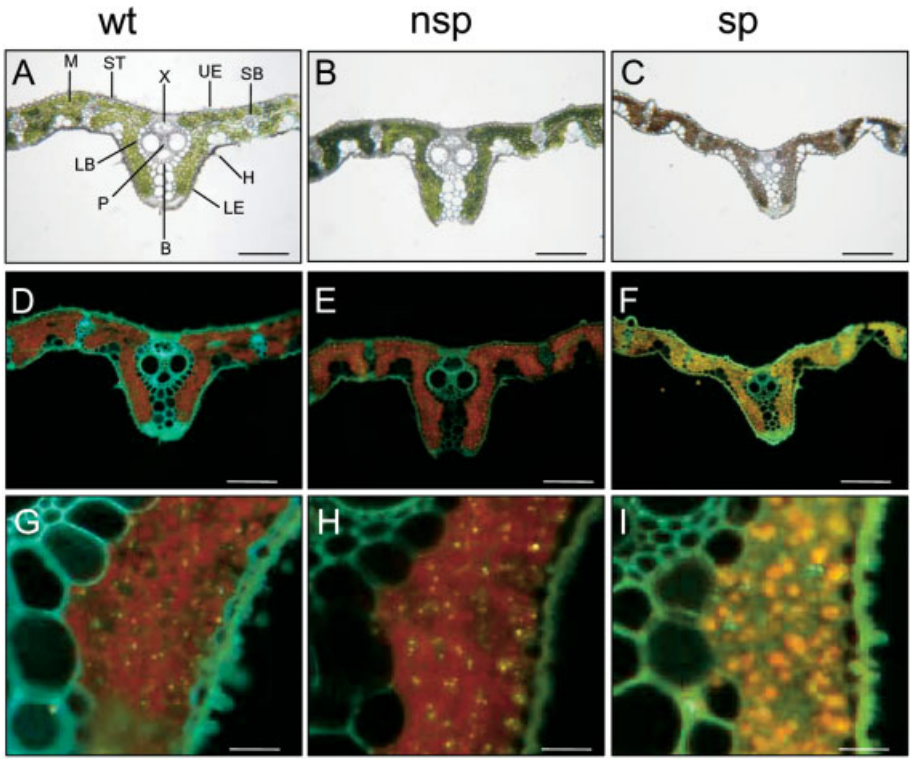

Figure 2. Light microscopy analysis of spotted and nonspl blades of *spl6* mutant and the wild-type leaf blades. Transverse sections observed under white light (A, B, and C) and observed under UV light at 488 nm (D, E, and F). G, H, and I are magnified view of small area of D, E, and F, respectively. A, D, and G are wild-type (wt) leaf sections. B, E, and H are nonspotted (nsp) and C, F, and I are spotted (sp) leaf sections of *spl6* mutant. Indications in A are LB, large vascular bundle; B, bundle sheath; LE, lower epidermis; P, phloem; S, small vascular bundle; ST, stomata; and UE, upper epidermis. Fully developed and matured leaf blades of wild type and mutant plants were used. Bars indicate 100 μm in A∼F and 25 μm in G∼I.

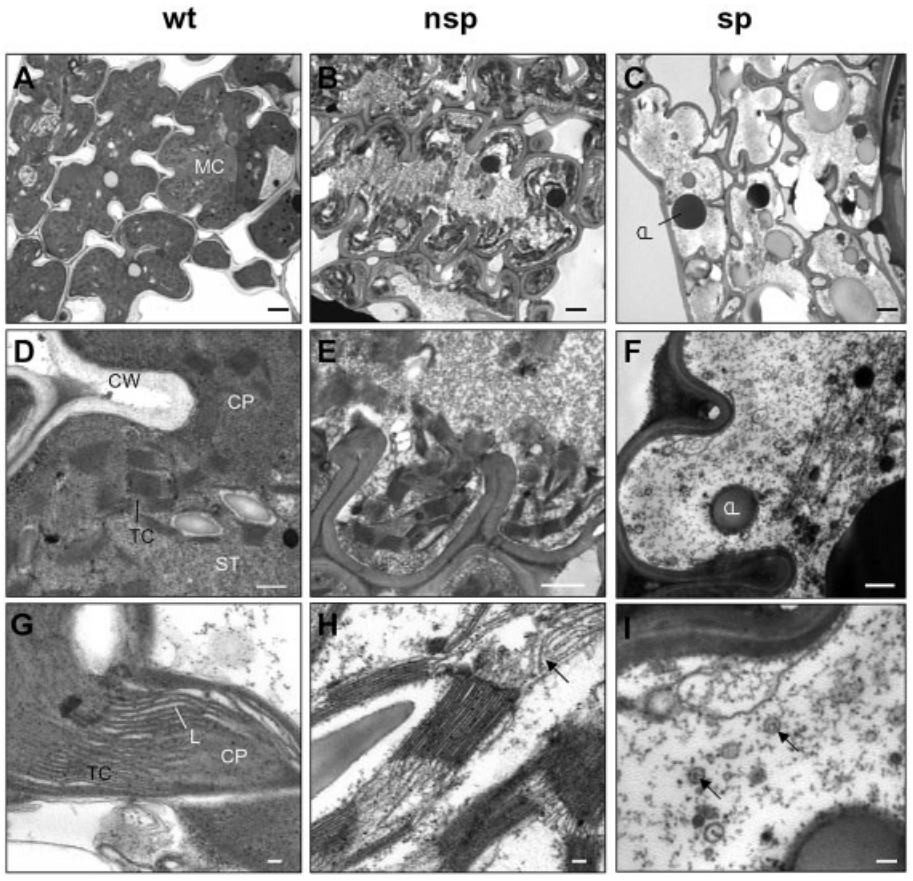

Figure 3. TEM analysis of wild type and *spl6* leaves. (A), (B), and (C) TEM analysis of the ultrastructure of chloroplasts of wild-type leaf blades (A), and nonspotted (nsp) (B), and spotted (sp) (C) leaf blades of *spl6* mutant. Close-ups of one chloroplast of wild type (D) and nonspotted (nsp) (E) and spotted (sp) (F) leaves of mutants. Close-ups of thylakoids with lamella of wild type (G), and nonspotted (nsp) (H), and spotted (sp), (I) of mutant leaves sections. Indications in the figures are CL, callose; CP, chloroplast; CW, chloroplast wall; L, lamella; MC, mesophyll chloroplast; TC, thylakoids, and ST, stroma. Arrow heads in the H and I indicate broken lamella and plastoglobules, respectively. Developed and matured flag leaves of the plants were used. Bars: A, B, and C, 2 μM; D, 0.5 μM; E, 2 μM; F, 0.5 μM; G, 0.1 μM; H, 0.1 μM; I, 2 μM.

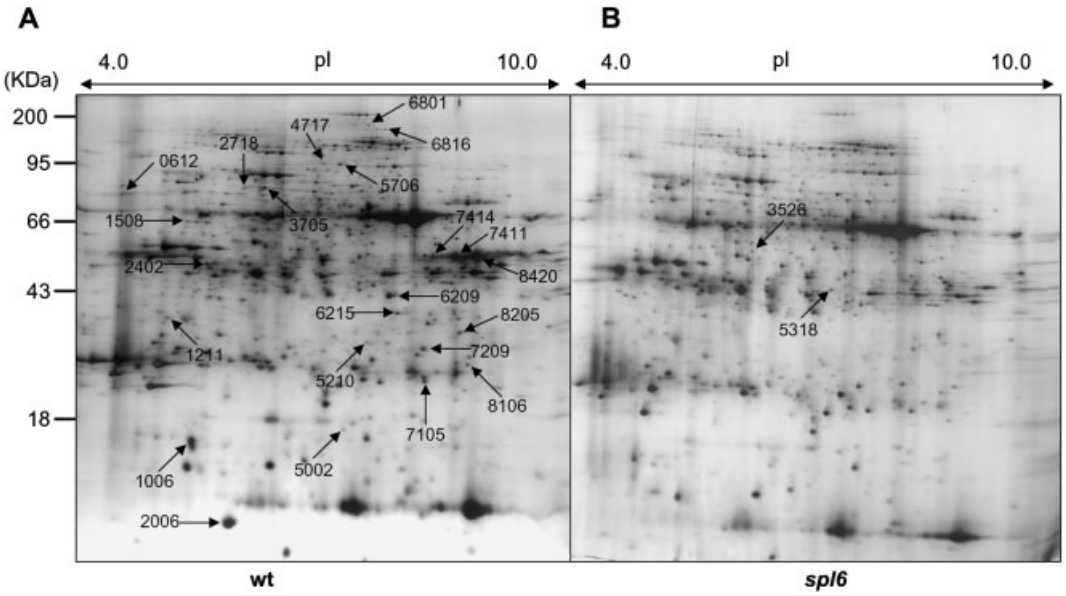

Figure 4. Representative 2-DE gel pattern of leaf blade proteins of wild type (wt) and *spl6* mutant. (A) 2-D gel pattern of wild type (wt) leaf proteins. (B) 2-D gel pattern of *spl6* leaf proteins. Arrow heads indicate more than twofold upregulated spots among the wild type and the mutant. IEF was performed with IPG dry strips (pH 4–10 NL, 24 cm length). SDS-PAGE was run in a 10–16% gradient SDS gel. After separation, the gels were stained with silver nitrate. Quantitative analysis of digitized images was carried out using the PDQuest software. Developed and matured leaf blades of 90-day-old plants were used to isolate proteins. Two independent experiments were performed.

into four functional categories including metabolism, photosynthesis, energy metabolism, and defense/stress response (http://www.kegg.com/) (Table 2).

We found that only the catalase (spot ID-5318) and one unknown protein, OSJNBa0020P07.1 (spot ID-3526), were upregulated in the *spl6* mutant compared with the wild type (Figs. 4B and 5; Table 2), whereas the other 23 spots, which represent nine annotated proteins including two unknown proteins, were either downregulated or absent in *spl6* mutant but were abundant in wild-type leaf proteins (Figs. 4A and 5; Table 2) These proteins are PDI, thioredoxin peroxidase (TPX), RuBisCO-ACS, transketolase (TK), ATPase α subunit, RuBisCO-L, ATPase α subunit from chloroplast insertion, chloroplast phosphoglycerate kinase (PGK), ATP synthase CF1 β chain and two unknown proteins, OSJNBa0020P07.3 and OSJNBa0074L08.12 (Table 2). After quantitative detection, the intensities of the spots were normalized by total valid spot intensity. The relative intensities of the spots expressed differentially between wild type and *spl6* are demonstrated in Fig. 5B.

3.4 Northern blot analysis

To confirm the protein expression patterns at the transcription level, we performed the Northern blot analysis. We found significant correlations of the levels of transcription with those of translations in wild type and *spl6* mutant (Fig. 6). Protein levels of RuBisCO-L, RuBisCO-ACS, PDI, and TPX were decreased in mutant plants but were abundant in wild type, whereas catalase was more abundant in mutant leaves when compared to wild-type leaves (Fig. 6A). However, transcription levels of RuBisCO-L, RuBisCO-ACS, PDI, and TPX genes were lower in the spotted leaves than the nonspotted leaves of *spl6* mutants as well as in wild-type leaves (Fig. 6B). Only the transcript levels of CAT gene were slightly increased in spotted leaves of *spl6* compared to that of the nonspl of *spl6* and the wild-type leaf (Fig. 6B).

4 Discussion

4.1 The *spl6* genetic trait is developmentally controlled

We observed the pattern of spot formation in all developmental stages of the *spl6* mutant (Fig. 1). In the *spl6* mutant plants, spots on the leaves appeared at the late tillering stage as very tiny specks and became clearly visible at the milk stage (90 days) (Fig. 1A), indicating that the pattern of spot formation is progressive toward developmental stages. Furthermore, because of severe spot formation on flag leaves, newly grown leaves, and seeds could not grow properly (Fig. 1A). This might have resulted from lower sucrose supplement due to malfunctioning photosynthesis in flag leaves.

The type of lesion formation in the *spl6* mutant is very similar to that in *spl3*, *spl4*, and *spl7* mutant rice [5, 19]. It has been reported that high temperature or UV solar radiation

Table 2. List of selected proteins differentially expressed between wild type and *spl6* mutant

Protein type	Spot id	Homologous protein	Source	Accession	MM	p*I*	Quantity		No. of peptide	Coverage (%)	EC No.
							wt	*spl6*			
Metabolism	0612	PDI	*O. sativa*	gi|7209794	72.48	4.40	821	0	16	31	EC 5.3.4.1
	2006	RuBisCO-L	*O. sativa*	gi|11466795	7.23	5.06	8624	499	6	9	EC 4.1.1.39
	5210	RuBisCO-L	*O. sativa*	gi|11466795	26.11	6.19	175	0	10	14	EC 4.1.1.39
	6215	RuBisCO-L	*O. sativa*	gi|11466795	32.24	6.62	659	0	21	22	EC 4.1.1.39
	7105	RuBisCO-L	*O. sativa*	gi|11466795	20.29	7.00	901	0	11	18	EC 4.1.1.39
	7209	RuBisCO-L	*O. sativa*	gi|11466795	24.96	6.99	730	0	11	19	EC 4.1.1.39
	7411	RuBisCO-L	*O. sativa*	gi|11466795	47.92	7.13	2265	413	19	25	EC 4.1.1.39
	7414	RuBisCO-L	*O. sativa*	gi|11466795	47.97	7.26	442	0	12	20	EC 4.1.1.39
	8420	RuBisCO-L	*O. sativa*	gi|11466795	47.83	7.77	394	65	19	26	EC 4.1.1.39
	1508	TK	*O. sativa*	gi|50933551	60.81	4.82	384	0	7	9	EC 2.2.1.1
	2718	TK	*O. sativa*	gi|50933551	75.15	5.14	197	0	5	8	EC 2.2.1.1
	3705	TK	*O. sativa*	gi|50933551	74.63	5.24	251	0	19	14	EC 2.2.1.1
	8106	TK	*O. sativa*	gi|50933551	22.26	7.63	287	0	7	8	EC 2.2.1.1
Photosynthesis	1211	RuBisCO-ACS	*O. sativa*	gi|8918361	31.16	4.69	414	0	18	24	NA
	5706	RuBisCo-ACS	*O. sativa*	gi|8918361	88.74	5.81	460	20	24	25	NA
	6209	RuBisCO-ACS	*O. sativa*	gi|8918361	36.45	6.49	1672	0	30	38	NA
Energy metabolism	2402	ATPase α subunit	*O. sativa*	gi|20143564	45.70	4.94	547	0	16	41	EC 3.6.3.14
	5002	ATP synthase CF1 β chain	*O. sativa*	gi|11466794	14.02	5.85	235	0	20	48	EC 3.6.3.14
	6816	ATPase α subunit from chloroplast insertion	*O. sativa*	gi|37533324	113.07	6.45	71	0	7	12	NA
	8205	PGK	*O. sativa*	gi|50931897	27.97	7.51	532	0	8	27	EC 2.7.2.3
Stress related	1006	TPX	*O. sativa*	gi|50252657	2.92	4.85	4690	0	6	30	EC 1.11.1.15
	5318	Catalase 1 (CAT)	*O. sativa*	gi|6635734	44.10	5.90	20	245	11	18	EC 1.11.1.6
Unknown	3526	OSJNBa0020P07.1	*O. sativa*	gi|32451277	54.74	5.29	3	131	7	12	NA
	4717	OSJNBa0020P07.3	*O. sativa*	gi|38344860	89.08	5.59	131	6	5	7	NA
	6801	OSJNBa0074L08.12	*O. sativa*	gi|38346621	116.84	6.21	126	0	6	8	NA

Note: Spot ID refers to the spot number as given in Figs. 4 and 5. Quantity refers to the average amount of proteins intensity of two independent analyses; MM, experimental molecular masses; p*I*, experimental isoelectric points; wt, wild type; No. of peptide, number of peptide sequenced; coverage %, the percentage of sequence coverage; EC No., SwissPort/UniPort identity number.

was the causal agent for the development of lesions on the surface of leaves of these mutants. Eventually, it was concluded that lesion development in *spl7* mutant was caused by dysfunction of a heat stress transcription factor protein (HSF) [5]. The predicted *spl6* locus is on chromosome 1 and tightly linked with the *lax* gene [27], whereas the *spl7* locus has been mapped at the end of the long arm of chromosome 7 [5]. Due to the differences of phenotypic, allelic as well as chromosomal location between *spl6* and *spl7*, we assume that the *spl6* mutant might be a different genetic mutation than *spl7* which is caused by a mutation of HSF. Therefore, further study is needed to conclude the exact molecular mechanism for the cause of the *spl6* mutation.

Furthermore, the pattern of spot formation in the *spl6* mutant was different from those in blast lesion 2 (*bl2*), blast lesion mimic (*blm*), and *spl5* mutant rice. Spots of *bl2* and *spl5* were observed at the early seedling stage and grew as large, dark circles along with the plant growth and became clearly visible on both sides of the leaf blade due to necrosis of the cells [19]. The lesions of *blm* mutant were initiated as small chlorotic spots and became straw colored necrotic lesions [21]. As we presented here, the pattern of spot formation on the leaf blades of *spl6* mutant was unique (Fig. 1B). Therefore, the *spl6* mutant characterized a different pattern of lesions than other *lrd* mutants.

Lesion formation on many of the identified *lrd* mutants in rice were found to be controlled by developmental processes as well as environmental factors including high-light intensity, some other abiotic stresses and senescence [3, 5, 19], whereas, we observed that spots of the *spl6* mutant started to form only at a certain developmental stage, indicating that the expression of the *spl6* genetic trait is developmentally programmed.

4.2 Chloroplast damage caused by oxidative burst creates lesions in *spl6* gene mutant

Light microscopic studies showed differences in the mesophyll cells between the *spl6* mutant and the wild-type plant, with the mutant having damaged chloroplasts (Figs. 2 and 3). Under light microscopy, the nonspl sections of *spl6* had similar green color in white light and similar red reflection

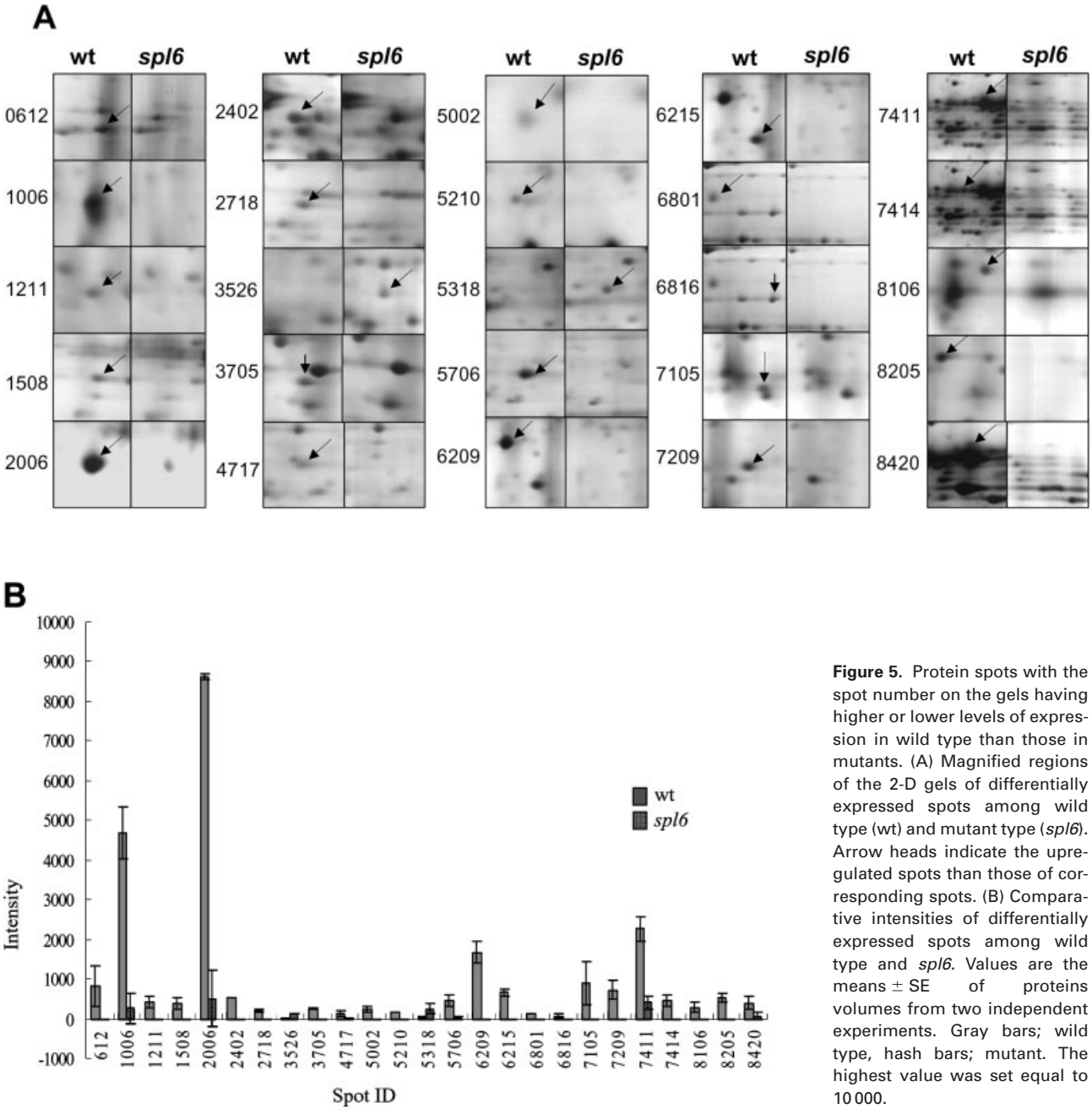

Figure 5. Protein spots with the spot number on the gels having higher or lower levels of expression in wild type than those in mutants. (A) Magnified regions of the 2-D gels of differentially expressed spots among wild type (wt) and mutant type (*spl6*). Arrow heads indicate the upregulated spots than those of corresponding spots. (B) Comparative intensities of differentially expressed spots among wild type and *spl6*. Values are the means ± SE of proteins volumes from two independent experiments. Gray bars; wild type, hash bars; mutant. The highest value was set equal to 10 000.

in UV-light to the wild type, indicating that chlorophyll molecules were still intact in the chloroplasts. However, spotted areas of the leaf of the *spl6* mutant showed lighter green color under white light and brown under UV light, indicating chloroplast damage in the mesophyll cells. Under TEM, damaged thylakoid membranes in the mesophyll chloroplasts were clearly observed in the nonspotted area of the *spl6* mutant (Fig. 3H). Furthermore, no chloroplasts were observed in the mesophyll cells from the spotted area of the *spl6* mutant (Fig. 3C). Instead, visible electron dense particles like plastoglobules were deposited in the mesophyll cells (Fig. 3I) which were similar to the results found in *A. thaliana*, where deposition of visible electron dense particles, plastoglobules, was found when the thylakoids accumulation was reduced in mutant plants [28]. However, our results indicate that the chloroplast damage was caused by an oxidative burst which creates excess substance deposition in the chloroplast as plastoglobules, as well as callose deposition (Figs. 3C, F, and I). These are the unique phenotypes of the *spl6* mutant among the identified lesion mimic mutants in rice.

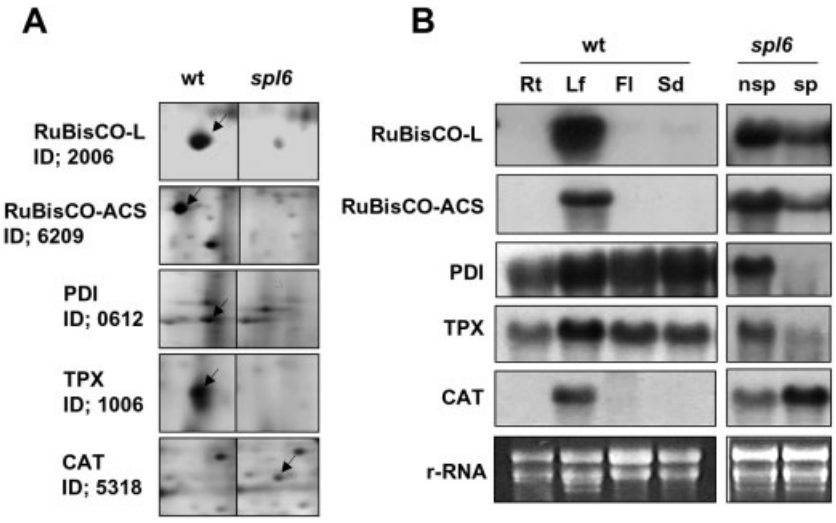

Figure 6. Confirmation of the differentially expressed five proteins in the *spl6* mutant and wild-type rice by Northern blot analysis. (A) Increased or decreased levels of PDI, spot ID 0612, TPX, ID 1006, RuBisCO-L, ID 2006, catalase (CAT, ID 5318), and RuBbisCO activase small isoform (RuBisCO-ACS, ID 6209) in wild type and *spl6* mutant. (B) Expression of PDI, TPX, RuBisCO-L, CAT, and RuBisCO-ACS at RNA level of wild type and *spl6* mutant. Proteins were extracted from matured leaf blade of wild-type rice (Ilpoom-byeo, YUC044) and *spl6* mutant. Total RNAs were extracted from roots (rt), leaves (lf), flowers (fl), and seeds (sd) of wild-type rice (Ilpoom-byeo, YUC044) as well as matured spotted (sp) and nonspotted (nsp) leaves of *spl6* mutants. Twenty micrograms of total RNAs were loaded in each lane. Ribosomal RNA bands are shown as loading control for each RNA blot. Arrow heads indicate the differentially expressed proteins. Two independent experiments were performed.

4.3 Selected proteins from proteome analysis may involve lesion development by oxidative burst

Proteome analysis of the *spl6* mutant provided clues to understand the PCD and to identify the functions of annotated proteins in lesion development. The quantitative data revealed that 23 protein spots were downregulated and two spots were upregulated in the *spl6* mutant compared to the wild type (Table 2). Further analysis revealed that among the analyzed protein spots, 22 spots represent ten annotated proteins and the other three spots were proteins of unknown function. Interestingly, most of the identified proteins were plastid-localized proteins. As we found chloroplast degradation was severe (Fig. 3), the identified proteins may be related directly or indirectly to lesion development in the *spl*6 mutant. Therefore, to predict the genes involved in lesion development of *spl6* mutant, we will discuss each protein function related to the oxidative burst.

4.3.1 Protein disulfide isomerase (spot ID 0612)

PDI is a cofactor in the folding of many proteins found in the lumen of ER of eukaryotic cells [29]. The major role of PDI is the formation and rearrangement of disulfide bonds in newly synthesized proteins through catalysis of oxidative folding. We found the reduced level of PDI in both the protein and RNA expression levels in the *spl6* mutant compared to the wild-type leaves (Fig. 5A and B). These results indicated that PDI no longer played role in the stabilization and facilitation of refolding the denatured proteins, during exposure to various stresses, which might result in the ultimate death of leaves. At low concentrations, PDI has been reported to show anti-chaperone activity where it facilitates aggregation of misfolded proteins [30]. PDI also functions in the purine, pyrimidine, and histidin metabolism through the pentose phosphate pathway (PPP) [31]. Therefore, we propose that the low concentrations of PDI protein in the *spl6* mutant leaves may not only reduce the purine and pyrimidine nucleotide synthesis from PPP but may also inhibit the protein disulfide bond formation and chaperone activity. These activities might result in inducing PCD.

4.3.2 Catalase (spot ID 5318)

CAT functions to protect cells from the toxic effects of hydrogen peroxide through decomposition of hydrogen peroxide to molecular oxygen and water. The antioxidant activity of CAT can protect plants from the toxic effects of ROS by reducing the activity and excessive production of ROS [2]. Among the identified proteins, only CAT was upregulated in both the protein and transcript levels of the *spl6* mutant, indicating that this mutant continuously produced CAT to protect the cell from the toxicity of ROS. In plant cells, this enzyme is located in leaf peroxisomes and glyoxysomes [32]. The upregulation of CAT in the *spl6* mutant suggested that the accumulation of ROS might be responsible for the lesion phenotype.

4.3.3 RuBisCO-L (spot ID 2006, 5210, 6215, 7105, 7209, 7411, 7414, and 8420)

RuBisCO-L is the key enzyme for photosynthetic carbon assimilation by catalyzing the reaction of CO_2 with ribulose 1,5-bisphosphate to form two molecules of D-phosphoglyceric acid (PGA) and it also catalyzes carbon oxidation in the stroma of the chloroplasts. It is the most abundant enzyme in the leaf. About 30% of total leaf proteins are RuBisCO [33]. However, we observed that this protein was downregulated and degraded to a different MM position in the protein gel compared with the expected size (50 kDa) in the wild type (Fig. 4, Table 2). These observations were similar to the results of degradation of RuBisCO by oxidative events [34, 35]. RuBisCO is known to be rapidly and selectively degraded during natural and stress-induced senescence and oxidative conditions have also been shown to expose RuBisCO to fragmentation at various MM positions [35]. Moreover, fragmentation of RuBisCO, caused by stress from fungal blast, has been observed to cause extensive formation of lesions [14] and fragmentation of RuBisCO-L into two smaller proteins has been observed as a result of bacterial blight in rice [36]. Therefore, as we predicted, fragmentation and degradation of RuBisCO-L might have occurred as a result of oxidative stresses in the *spl6* mutant.

4.3.4 RuBisCO-ACS (spot ID 1211, 5706, and 6209)

RuBisCO-ACS activates RuBisCO and involves the ATP-dependent carboxylation of the epsilon-amino group of lysine leading to a carbamate structure [37]. It is abundant mostly in the chloroplasts. Like RuBisCO-L, the reduction of RuBisCO-ACS protein and its gene expression in the *spl6* mutant might have resulted by either the malfunctioning of photosynthesis or degradation of chloroplasts.

4.3.5 Transketolase (spot ID 1508, 2718, 3705, and 8106)

TK is an enzyme of the Calvin cycle of photosynthesis and the PPP. TK participates in the fixation of carbon dioxide which catalyzes the reversible transfer of a two-carbon ketol group from fructose-6-phosphate or sedoheptulose-7-phosphate to glyceraldehyde-3-phosphate to yield xylulose-5-phosphate and erythrose-4-phosphate or ribose-5-phosphate, respectively [38]. It has been reported that decreasing TK inhibits ribulose-1,5-bisphosphate regeneration and photosynthesis and resulted in loss of chlorophyll [39]. We also observed that TK was not found in the *spl6* mutant (Table 2), indicating that the reduced level of TK in *spl6* might have resulted in chloroplast degradation and lesion development.

4.3.6 Phosphoglycerate kinase (spot ID 8205)

Chloroplast phosphoglycerate kinase (PGK) has a role in the reduction phase of the Calvin cycle and in carbohydrate biosynthesis [40]. It has been found in the stroma of chloroplasts, where it functions in catalyzing the reversible, ATP-dependent conversion of 3-phosphoglycerate to 1,3-diphosphoglycerate [41]. Downregulation of this protein was found in *spl6* mutant plants compared with wild-type plants, indicating that chloroplast degradation in lesion development resulted in the reduction of this protein.

4.3.7 ATPase α subunit and ATP synthase CF1 β chain (spot ID 2402 and 5002, respectively)

ATP synthase produces ATP from ADP in the presence of a proton gradient across the membrane [42]. ATP synthase contains the catalytic site for ATP synthesis during photooxidative phosphorylation in the chloroplast [43]. These proteins were not identified in leaves of the *spl6* mutant (Table 2). We also observed that the thylakoid membrane, which is the location of ATP synthase, was severely degraded when lesions developed in the *spl6* mutant (Fig. 3). Therefore, the reduction of ATP synthase probably resulted from thylakoid membrane damage caused by ROS in the oxidative burst.

4.3.8 Thioredoxin peroxidase (TPX) (spot ID 1006)

This multifunctional protein is involved in intracellular redox signaling which reduces hydrogen peroxide (H_2O_2) to water and alkyl hydroperoxides to the corresponding alcohol [44]. When rice plants are exposed to stresses, such as pathogen attack, high-salt concentrations, mechanical damage, and chilling, large amounts of ROS are generated. The plant's superoxide dismutase, catalase, and a large family of antioxidant enzymes, including glutathione peroxidase (GPX), ascorbate peroxidase (APX), peroxidase, glutathione reductase (GR), glutathoine-*S*-transferase (GST), and TPX, protect the chloroplasts against oxidative damage by reducing ROS [45]. It has been reported that NADPH thioredoxin reductase (NTRC) deficient plants produce an increase in hydrogen peroxide and lipid peroxidation in leaves and accelerate senescence in *A. thaliana* [46]. Here, we found the absence of TPX both in mRNA and protein levels in the *spl6* mutant (Figs. 5A and B). Like the NTRC-deficient mutant, TPX deficiency in the *spl6* mutant might cause the increased level of hydrogen peroxide that ruptures the membrane structures resulting in cell death and senescence.

Findings presented in this study suggest that reduction of TPX gene expression in the *spl6* mutant failed to protect cells from ROS by oxidative burst, resulting in thylakoid membrane degradation leading to PCD and development of lesions in the *spl6* mutant. In addition, lack of PDI protein may reduce the amount of nucleotide production through PPP and limit chaperone activity, resulting in the induction of PCD. We observed that many physiological and biological changes caused by malfunction of the *spl6* gene may take place during cell death in the *spl6* mutant, including breakage of chloroplasts, rupture of cytoplasmic membranes and tonoplast, and degradation of cell organelles. Thus, further

studies of the genetic function and mechanism of the *spl6* gene in the lesion mimic mutants will achieve a fundamental understanding of the genetic causes and regulatory processes of PCD and resistance against pathogenic stresses.

We thank Dr. Hak Soo Suh, Dr. Sung Soo Kim, and Devendra Pandeya at Yeungnam University, Gyeongsan, Korea, for growing rice. We also thank Dr. Dong Soo Kim, Dr. Won Man Park, and Dr. Hyeong Jin Na at Genomine Co., Pohang, Korea, for their technical assistance for the proteomics and Dr. Marshall Elson, USDA/ARS, Plant Sciences Institute, Beltsville, Maryland, USA, for editing and discussions. This research was supported by a grant (CG2113) from the Crop Functional Genomics Center of the 21st Century Frontier Research Program funded by the Ministry of Science and Technology of the Republic of Korea.

5 References

[1] Mehta, R. A., Fawcett, T. W., Porath, D., Mattoo, A. K., *J. Biol. Chem.* 1992, *267*, 2810–2816.

[2] Scandalios, J. G., in: Scandalios, J. G. (Ed.), *Molecular Biology of free Radical Scavenging Systems*, Cold Spring Harbor Laboratory Press, New York 1992, pp. 117–152.

[3] Yin, Z., Chen, J., Zeng, L., Goh, M. *et al.*, *Mol. Plant Microbe Interact.* 2000, *13*, 869–876.

[4] Kerr, J. F. R., Wyllie, A. H., Currie, A. R., *Br. J. Cancer* 1972, *26*, 239–257.

[5] Yamanouchi, U., Yano, M., Lin, H., Ashikari, M., Yamada, K., *Proc. Natl. Acad. Sci. USA* 2002, *99*, 7530–7535.

[6] Tomiyama, K., *Annu. Rev. Phytopathol.* 1963, *1*, 295–324.

[7] Greenberg, J. T., Ausubel, F. M., *Plant J.* 1993, *4*, 327–341.

[8] Balague, C., Lin, B., Alcon, C., Flottes, G. *et al.*, *Plant Cell* 2003, *15*, 365–379.

[9] Liu, G., Wang, L., Zhou, Z., Leung, H. *et al.*, *Mol. Genet. Genomics* 2004, *272*, 108–115.

[10] Kiyosawa, S., *Bull. Nat. Inst. Agric. Sci. (Jpn.) Ser. D. Physiol. Genet.* 1970, *21*, 61–71.

[11] Hoisington, D. A., Neuffer, M. G., Walbot, V., *Dev. Biol.* 1982, *93*, 381–388.

[12] Wolter, M., Hollricher, K., Salamini, F., Schilze-Lefert, P., *Mol. Gen. Genet.* 1993, *239*, 122–128.

[13] Lorrian, S., Vailleau, F., Balague, C., Roby, D., *Trends Plant Sci.* 2003, *8*, 263–271.

[14] Tsunezuka, H., Fujiwara, M., Kawasaki, T., Shimamoto, K., *Mol. Plant Microbe Interact.* 2005, *18*, 52–59.

[15] Dietrich, R. A., Richberg, M. H., Schmidt, R., Dean, C., Dangl, J. L., *Cell* 1997, *88*, 685–694.

[16] Buschges, R., Hollricher, K., Panstruga, R., Simons, G. *et al.*, *Cell* 1997, *7*, 695–705.

[17] Hu, G., Yalpani, N., Briggs, S. P., Johal, G. S., *Plant cell* 1998, *10*, 1095–1105.

[18] Kinoshita, T., *Rice Genet. Newsl.* 1995, *12*, 9–115.

[19] Matin, M. N., Suh, H. S., Kang, S. G., *Korean J. Genet.* 2006, *28*, 221–228.

[20] Takahashi, A., Kawasaki, T., Wong, H. L., Suharsono, U. *et al.*, *Plant Physiol.* 2003, *132*, 1861–1869.

[21] Jung, Y. H., Lee, J. H., Agrawal, G. K., Rakwal, R. *et al.*, *Plant Physiol. Biochem.* 2005, *43*, 397–406.

[22] Zeng, L. R., Qu, S., Bordeos, A., Yang, C. *et al.*, *Plant Cell* 2004, *16*, 2795–2808.

[23] Bradford, M. M., *Anal. Biochem.* 1976, *72*, 248–254.

[24] Oakley, B. R., Kirsch, D. R., Morris, N. R., *Anal. Biochem.* 1980, *105*, 361–363.

[25] Shevchenko, A., Wilm, M., Vorm, O., Mann, M., *Anal. Chem.* 1996, *68*, 850–858.

[26] Kang, S. G., Jeong, H. K., Suh, H. S., *Mol. Cells* 2004, *17*, 23–28.

[27] Kishimoto, N., Shimosaka, E., Matsuura, S., Saito, A., *Rice Genet. Newsl.* 1992, *9*, 118–124.

[28] Rudella, A., Friso, G., Alonso, J. M., Ecker, J. R., van Wijk, K. J., *Plant Cell* 2006, *18*, 1704–1721.

[29] Gilbert, H. F., *J. Biol. Chem.* 1997, *272*, 29399–29402.

[30] Puig, A., Gilbert, H. F., *J. Biol. Chem.* 1994, *269*, 7764–7771.

[31] Bulleid, N. J., *Adv. Protein Chem.* 1993, *44*, 125–150.

[32] Beevers, H., *Annu. Rev. Plant Physiol.* 1979, *30*, 159–193.

[33] Ellis, R. J., *Trends Biochem. Sci.* 1979, *4*, 241–244.

[34] Nozu, Y., Tsugita, A., Kamijo, K., *Proteomics* 2006, *6*, 3665–3670.

[35] Penarrubia, L., Moreno, J., *Arch. Biochem. Biophys.* 1990, *281*, 319–323.

[36] Mahmood, T., Jan, A., Kakishima, M., Komatsu, S., *Proteomics* 2006, *6*, 6053–6065.

[37] Salvucci, M. E., Crafts-Brandner, S. J., *Plant Physiol.* 2004, *134*, 1460–1470.

[38] Schenk, G., Duggleby, R. G., Nixon, P. F., *Int. J. Biochem. Cell Biol.* 1998, *30*, 1297–1318.

[39] Henkes, S., Sonnewald, U., Badur, R., Flachmann, R., Stitt, M., *Plant Cell* 2001, *13*, 535–551.

[40] Majeran, W., Cai, Y., Sun, Q., van Wijk, K. J., *Plant Cell* 2005, *17*, 3111–40.

[41] Jones, P. G., Raines, C., Lloyd, J. C., *Plant Physiol.* 1995, *107*, 1483–1484.

[42] Tucker, W. C., Du, Z., Hein, R., Gromet-Elhanan, Z., Richter, M. L., *Biochemistry* 2001, *26*, 7542–7548.

[43] Jiao, S., Hilaire, E., Guikema, J. A., *Plant Physiol. Biochem.* 2004, *42*, 883–890.

[44] Schröder, E., Pointing, C. P., *Protein Sci.* 1998, *7*, 2465–2468.

[45] Hiraga, S., Sasaki, K., Ito, H., Ohashi, Y., Matsui, H., *Plant Cell Physiol.* 2001, *42*, 462–468.

[46] Perez-Ruiz, J. M., Spinola, M. C., Kirchsteiger, K., Moreno, J. *et al.*, *Plant Cell* 2006, *18*, 2356–2368.

